

cipitated beads were resuspended in 23 μ l lysis buffer and aliquoted as indicated.

Histone deacetylase assays. Assays were done as described¹; where indicated, ATP was added to 2.5 mM in the presence of 5 mM MgCl₂, and trapoxin was added to 200 nM.

8-azido-adenosine- γ -³²P-ATP crosslinking. NRD antibody-immobilized bead complexes were incubated with 2 μ Ci 8-azido-adenosine-5'- γ -³²P-triphosphate (ICN) for 3 min at room temperature in 50 μ l buffer containing 20 mM HEPES, pH 7.6, 100 mM KCl, 5 mM MgCl₂, 1 μ M ZnSO₄, 0.1% Tween-20. The reaction mixture was irradiated for 5 min with 254-nm UV light (1,120 μ W cm⁻² from 3 cm away). Beads were washed three times with 1 ml 20 mM HEPES, pH 7.6, 100 mM KCl, 0.1% Tween-20. Bound proteins were resolved by SDS-PAGE and imaged using a phosphorimager.

Nucleosome-disruption assays. the 155-bp pTPT *MluI/EcoRI* fragment was prepared and footprinted as described¹³. 0.2, 1.0 and 5.0 μ l HDAC/CHD immunoprecipitates, 1.0 and 5.0 μ l peptide-blocked HDAC/CHD immunoprecipitates, and 0.04, 0.16, 0.6 and 2.4 μ l of hSWI/SNF were tested for disruptive activity. 2 mM ATP/MgCl₂ was added where indicated; after 45 min, reactions were treated with 0.12 U DNase I (0.012 U for bare DNA).

Plasmid chromatin reconstitution. HeLa cells were radiolabelled as described previously⁴ and hyperacetylated histones were purified by hydroxyapatite chromatography as described¹⁴. 16 μ g of a 9-kb plasmid was linearized, purified, and mixed with an equal mass of radiolabelled, hyperacetylated core histones in 50 μ l of 15 mM HEPES, pH 7.5, 1 M NaCl, 0.2 mM EDTA and 0.2 mM PMSF. Stepwise dilution of salt was done by addition of the same buffer without NaCl over 3 h at 10-min intervals until the final concentration of NaCl was 100 mM. Non-nucleosomal histones were then separated by repeat Centricon-500 (Amicon) filtration. Nucleosomal structure was confirmed by micrococcal nuclease digestion of the product.

Received 24 August; accepted 28 September 1998.

- Elgin, S. C. R. *Chromatin Structure and Gene Expression* (eds Hames, B. D. & Glover, D. M.) (IRL, Oxford, 1995).
- Pazin, M. J. & Kadonaga, J. T. SWI2/SNF2 and related proteins: ATP-driven motors that disrupt protein-DNA interactions? *Cell* **88**, 737-740 (1997).
- Imhof, A. & Wolffe, A. P. Transcription: gene control by targeted histone acetylation. *Curr. Biol.* **8**, R422-424 (1998).
- Hassig, C. A. *et al.* A role for histone deacetylase activity in HDAC1-mediated transcriptional repression. *Proc. Natl Acad. Sci. USA* **95**, 3519-3524 (1998).
- Wade, P. A., Jones, P. L., Vermaak, D. & Wolffe, A. P. A multiple subunit Mi-2 histone deacetylase from *Xenopus laevis* cofractionates with an associated Snf2 superfamily ATPase. *Curr. Biol.* **8**, 843-846 (1998).
- Tavladoraki, P. *et al.* Maize polyamine oxidase—primary structure from protein and cDNA sequencing. *FEBS Lett.* **426**, 62-66 (1998).
- Seelig, H. P. *et al.* The major dermatomyositis-specific Mi-2 autoantigen is a presumed helicase involved in transcriptional activation. *Arthr. Rheum.* **38**, 1389-1399 (1995).
- Ge, Q., Nilasena, D. S., O'Brien, C. A., Frank, M. B. & Targoff, I. N. Molecular analysis of a major antigenic region of the 240-kD protein of Mi-2 autoantigen. *J. Clin. Invest.* **96**, 1730-1737 (1995).
- Woodage, T., Basrai, M. A., Baxevarian, A. D., Hieter, P. & Collins, F. S. Characterization of the CHD family of proteins. *Proc. Natl Acad. Sci. USA* **94**, 11472-11477 (1997).
- Hartzog, G. A. & Winston, F. Nucleosomes and transcription: recent lessons from genetics. *Curr. Opin. Genet. Dev.* **7**, 192-198 (1997).
- Kadonaga, J. T. Eukaryotic transcription: an interlaced network of transcription factors and chromatin-modifying machines. *Cell* **92**, 307-313 (1998).

- De Rubertis, F. *et al.* The histone deacetylase RPD3 counteracts genomic silencing in *Drosophila* and yeast. *Nature* **384**, 589-591 (1996).
- Schnitzler, G., Sif, S. & Kingston, R. E. Human SWI/SNF interconverts a nucleosome between its base state and a stable remodeled state. *Cell* **94**, 17-27 (1998).
- Cote, J., Utley, R. T. & Workman, J. L. Basic analysis of transcription factor binding to nucleosomes. *Meth. Mol. Genet.* **6**, 108-128 (1995).

Acknowledgements. We thank W. Wang for unpublished CHD3 and CHD4 antisera and for sharing unpublished results; I. Targoff for human Mi-2-positive antiserum and rabbit anti-Mi-2 α antiserum; W. Lane and colleagues at the Harvard Microsequencing Facility for peptide microsequencing; O. Rando, C. Grozinger, D. Ayer, and I. Wilson for discussion; and the NIH Cell Culture Center for technical assistance. This work was supported by a National Institute of General Medical Sciences grant to S.L.S. and an NIH grant to R.E.K. G.R.S. is a Helen Hay Whitney Fellow. Predoctoral fellowships from the NSF and the Harvard-Markey Biomedical Scientist Program to J.K.T. and an NIH predoctoral training grant to C.A.H. are gratefully acknowledged. S.L.S. is an Investigator of the Howard Hughes Medical Institute.

Correspondence and requests for materials should be addressed to S.L.S. (e-mail: sls@slsirir.harvard.edu).

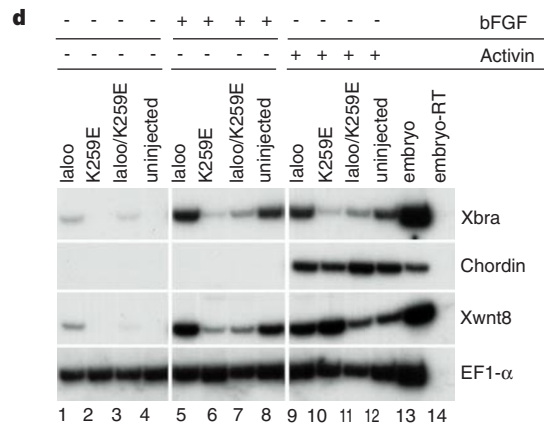
erratum

FGF-mediated mesoderm induction involves the Src-family kinase Laloo

Daniel C. Weinstein, Jennifer Marden, Francesca Carnevali & Ali Hemmati-Brivanlou

Nature **394**, 904-908 (1998)

In Fig. 4d of this Letter, it was wrongly indicated that activin was added to samples 5-8. Activin was not added to these samples but to samples 9-12 as shown here.



described²⁸. IL-2 production was measured by enzyme-linked immunosorbent assay (ELISA) with the monoclonal antibodies JES6-1A12 and JES6-5H4 (Pharmingen). Purified naive splenic CD4 cells were differentiated into Th1 cells as described²⁹ or with PMA plus A23187. Briefly, 10⁶ CD4 cells were stimulated with 5 ng ml⁻¹ PMA (Calbiochem), 100 ng ml⁻¹ A23187 (Calbiochem) and 1.5 ng ml⁻¹ IL-12 (R&D, Wiesbaden). After 4 days of culture, cells were restimulated with PMA plus A23187 and analysed for intracellular cytokine expression²⁹.

Western blot analysis and *in vitro* kinase assays. Cells were lysed in 1% NP-40 lysis buffer (10 mM Tris/HCl, pH 7.8, 150 mM NaCl, 4 mM EDTA, 10% glycerol, 2 mM Na₃VO₄, 100 mM NaF, 2 µg ml⁻¹ aprotinin, 1 µg ml⁻¹ leupeptin, 1 mM PMSF). Lysates were resolved by 10% SDS-PAGE and transferred to PVDF membrane (Immobilon-P, Millipore). Membranes were incubated with anti-Csk (Santa Cruz), anti-α-tubulin (DM1A, Sigma), anti-Lck (CT, UBI, Lake Placid) or anti-Fyn (FYN3, Santa Cruz) antibodies and proteins were detected by chemiluminescence (SuperSignal, Pierce). For *in vitro* kinase assays, NP-40 lysates of 5 × 10⁷ thymocytes were precipitated with anti-Lck (3A5, UBI) or anti-Fyn (FYN15, Santa Cruz) antibodies and protein-A sepharose. Immune complexes were incubated in kinase buffer (10 mM HEPES, pH 7.4, 5 mM MgCl₂, 5 mM MnCl₂) with 15 µCi[γ-³²P]ATP for 2 min at 37 °C and resolved by 10% SDS-PAGE. The conditions of the kinase assay were tested to fall within the linear range of the kinase reaction. Autophosphorylation of Lck and Fyn was quantified by phosphorimage analysis of dried gels with Fuji Bas1000.

Received 5 June; accepted 8 July 1998.

1. von Boehmer, H. & Fehling, H. J. Structure and function of the pre-T cell receptor. *Annu. Rev. Immunol.* **15**, 432–452 (1997).
2. Mombaerts, P. Lymphocyte development and function in T-cell receptor and RAG-1 mutant mice. *Int. Rev. Immunol.* **13**, 43–63 (1995).
3. Alberola-Ila, J., Takaki, S., Kerner, J. D. & Perlmutter, R. M. Differential signaling by lymphocyte antigen receptors. *Annu. Rev. Immunol.* **15**, 125–154 (1997).
4. Weiss, A. & Littman, D. R. Signal transduction by lymphocyte antigen receptors. *Cell* **76**, 263–274 (1994).
5. Nada, S., Okada, M., MacAuley, A., Cooper, J. A. & Nakagawa, H. Cloning of a complementary DNA for a protein-tyrosine kinase that specifically phosphorylates a negative regulatory site of p60^{src}. *Nature* **351**, 69–72 (1991).
6. Jameson, S. C., Hogquist, K. A. & Bevan, M. J. Positive selection of thymocytes. *Annu. Rev. Immunol.* **13**, 93–126 (1995).
7. Groves, T. *et al.* Fyn can partially substitute for Lck in T lymphocyte development. *Immunity* **5**, 417–428 (1996).
8. van Oers, N. S., Lowin-Kropf, B., Finlay, D., Connolly, K. & Weiss, A. αβ T cell development is abolished in mice lacking both Lck and Fyn protein tyrosine kinases. *Immunity* **5**, 429–436 (1996).
9. Mombaerts, P., Anderson, S. J., Perlmutter, R. M., Mak, T. W. & Tonegawa, S. An activated lck transgene promotes thymocyte development in RAG-1 mutant mice. *Immunity* **1**, 261–267 (1994).
10. Nada, S. *et al.* Constitutive activation of Src family kinases in mouse embryos that lack Csk. *Cell* **73**, 1125–1135 (1993).
11. Imamoto, A. & Soriano, P. Disruption of the csk gene, encoding a negative regulator of Src family tyrosine kinases, leads to neural tube defects and embryonic lethality in mice. *Cell* **73**, 1117–1124 (1993).
12. Hanks, S. K. & Hunter, T. Protein kinases 6. The eukaryotic protein kinase superfamily: kinase (catalytic) domain structure and classification. *FASEB J.* **9**, 576–596 (1995).
13. Kühn, R., Schwenk, F., Aguet, M. & Rajewsky, K. Inducible gene targeting in mice. *Science* **269**, 1427–1429 (1995).
14. Moore, T. A., von Freeden-Jeffry, U., Murray, R. & Zlotnik, A. Inhibition of gamma delta T cell development and early thymocyte maturation in IL-7^{-/-} mice. *J. Immunol.* **157**, 2366–2373 (1996).
15. Mombaerts, P. *et al.* Mutations in T-cell antigen receptor genes α and β block thymocyte development at different stages. *Nature* **360**, 225–231 (1992).
16. Wilson, A., Day, L. M., Scollay, R. & Shortman, K. Subpopulations of mature murine thymocytes: properties of CD4⁺CD8⁺ and CD4⁺CD8⁻ thymocytes lacking the heat-stable antigen. *Cell Immunol.* **117**, 312–326 (1988).
17. Swat, W., Dessing, M., von Boehmer, H. & Kisielow, P. CD69 expression during selection and maturation of CD4⁺8⁺ thymocytes. *Eur. J. Immunol.* **23**, 739–746 (1993).
18. Sprent, J. & Tough, D. F. Lymphocyte life-span and memory. *Science* **265**, 1395–1400 (1994).
19. Vellette, A., Bookman, M. A., Horak, E. M. & Bolen, J. B. The CD4 and CD8 T cell surface antigens are associated with the internal membrane tyrosine-protein kinase p56^{lck}. *Cell* **55**, 301–308 (1988).
20. Norment, A. M., Forbush, K. A., Nguyen, N., Malissen, M. & Perlmutter, R. M. Replacement of pre-T cell receptor signaling functions by the CD4 coreceptor. *J. Exp. Med.* **185**, 121–130 (1997).
21. Köntgen, F., Suss, G., Stewart, C., Steinmetz, M. & Bluethmann, H. Targeted disruption of the MHC class II α gene in C57BL/6 mice. *Int. Immunol.* **5**, 957–964 (1993).
22. Grusby, M. J., Johnson, R. S., Papaioannou, V. E. & Glimcher, L. H. Depletion of CD4⁺ T cells in major histocompatibility complex class II-deficient mice. *Science* **253**, 1417–1420 (1991).
23. Gosgrove, D. *et al.* Mice lacking MHC class II molecules. *Cell* **66**, 1051–1066 (1991).
24. Torres, R. & Kühn, R. *Laboratory Protocols for Conditional Gene Targeting* (Oxford Univ. Press, 1997).
25. Ledbetter, J. A. & Herzenberg, L. A. Xenogeneic monoclonal antibodies to mouse lymphoid differentiation antigens. *Immunol. Rev.* **47**, 63–90 (1979).
26. Anderson, S. J., Abraham, K. M., Nakayama, T., Singer, A. & Perlmutter, R. M. Inhibition of T-cell receptor β-chain gene rearrangement by overexpression of the non-receptor protein tyrosine kinase p56^{lck}. *EMBO J.* **11**, 4877–4886 (1992).
27. Krotkova, A., von Boehmer, H. & Fehling, H. J. Allelic exclusion in pTα-deficient mice: no evidence for cell surface expression of two T cell receptor (TCR)-β chains but less efficient inhibition of endogenous Vβ → (D)Jβ rearrangements in the presence of a functional TCR-β transgene. *J. Exp. Med.* **186**, 767–775 (1997).
28. Saijo, K., Park, S. Y., Ishida, Y., Arase, H. & Saito, T. Crucial role of Jak3 in negative selection of self-reactive T cells. *J. Exp. Med.* **185**, 351–356 (1997).
29. Murphy, E. *et al.* Reversibility of T helper 1 and 2 populations is lost after long-term stimulation. *J. Exp. Med.* **183**, 901–913 (1996).

Acknowledgements. We thank A. Berns and H. Jacobs for TCRβ^{-/-} mice; H. Bluethmann and I. Förster for Act^{-/-} mice; D. Loh and M. Löhning for DO11.10 mice; C. Göttlinger, B. Meiners, S. Irlenbusch and C. Uthoff-Hachenberg for technical assistance; and J. Howard and K. Rajewsky for discussions and critical reading of the manuscript. This work was supported by the Deutsche Forschungsgemeinschaft through SFB 243. C.S. was supported by the Fonds der Chemie. K.S. was supported by an EMBO long-term fellowship.

Correspondence and requests for material should be addressed to C.S. (e-mail: c.schmedt@uni-koeln.de) and A.T. (e-mail: sasha@mac.genetik.uni-koeln.de).

FGF-mediated mesoderm induction involves the Src-family kinase Laloo

Daniel C. Weinstein, Jennifer Marden, Francesca Carnevali* & Ali Hemmati-Brivanlou

Department of Molecular Vertebrate Embryology, The Rockefeller University, 1230 York Avenue, New York, New York 10021, USA

During embryogenesis, inductive interactions underlie the development of much of the body plan. In *Xenopus laevis*, factors secreted from the vegetal pole induce mesoderm in the adjacent marginal zone; members of both the transforming growth factor-β (TGF-β) and fibroblast growth factor (FGF) ligand families seem to have critical roles in this process¹. Here we report the identification and characterization of *laloo*, a novel participant in the signal transduction cascade linking extracellular, mesoderm-inducing signals to the nucleus, where alteration of cell fate is

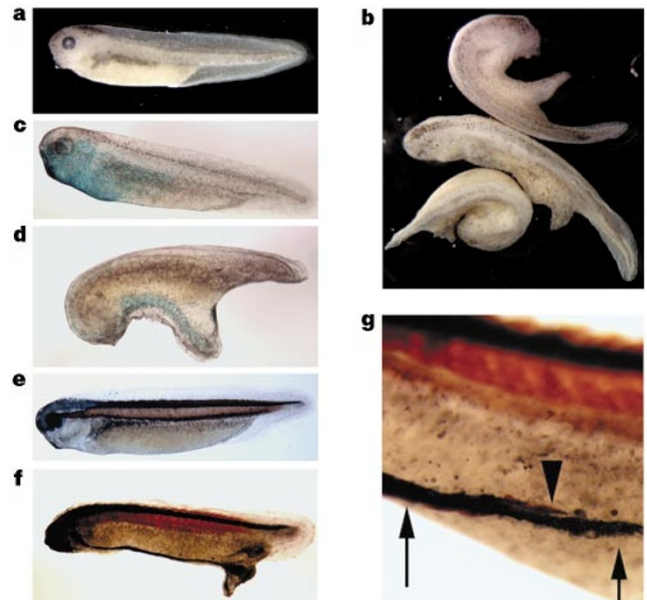


Figure 1 Effects of injection of *laloo* into embryos. Embryos were injected with 100 pg β-galactosidase RNA (c, d) and/or 750 pg (b, d, f, g) 27A1JA (*laloo*) RNA. All embryos are stage 33–35. **a**, Uninjected embryo. **b**, Dorsal view of embryos injected with 27A1JA. **c**, Embryo injected with β-galactosidase (β-Gal) RNA and stained with 5-bromo-4-chloro-3-indolyl-β-D-galactoside (X-gal) as a substrate. **d**, Embryo co-injected with 27A1JA and β-Gal RNA, and stained with X-gal as a substrate. **e–g**, Lateral views of embryos probed with neural-specific (blue stain) (6F11 (ref. 27)) and somite-specific (red stain) (12/101 (ref. 28)) antibodies. **e**, Uninjected embryo. **f, g**, Embryo injected with 27A1JA RNA. Panel **g** is a detail of the trunk of embryo in **f**; arrows indicate ectopic neural tissue, arrowhead indicates ectopic mesoderm. Embryos in **c–g** were cleared in 2:1 benzyl benzoate/benzyl alcohol.

* Present address: Centro di Studio per gli Acidi Nucleici, CNR, Università di Roma La Sapienza, P.le Aldo Moro n. 5, 00185 Roma, Italy.

driven by changes in gene expression. Overexpression of *laloo*, a member of the Src-related gene family, in *Xenopus* embryos gives rise to ectopic posterior structures that frequently contain axial tissue. *Laloo* induces mesoderm in *Xenopus* ectodermal explants; this induction is blocked by reagents that disrupt the FGF signalling pathway. Conversely, expression of a dominant-inhibitory *Laloo* mutant blocks mesoderm induction by FGF and causes severe posterior truncations *in vivo*. This work provides the first evidence that a Src-related kinase is involved in vertebrate mesoderm induction.

In an attempt to isolate factors involved in patterning of the body axis, we constructed and screened a *Xenopus* gastrula expression library. Early cleavage stage embryos were injected in the animal pole with RNA from fractionated library pools. One clone, 27AIJA, generated ectopic structures that resemble tails in over 90% of injected embryos ($n = 102$) (Fig. 1a, b). In addition, a reduction of anterior structures, including eyes, was often observed (Fig. 1, and not shown). Co-injection of 27AIJA and β -Gal RNA revealed that injected cells contribute directly to ectopic structures (Fig. 1c, d). Whole-mount immunohistochemistry demonstrated that these ectopic structures often contain neural tissue (17 out of 32 embryos) and paraxial mesoderm (5 out of 32 embryos) (Fig. 1e–g). Thus, overexpression of 27AIJA generates ectopic, posterior structures that frequently contain axial and paraxial tissue.

The 27AIJA cDNA contains an open reading frame of 496 amino

acids (Fig. 2a); this sequence shows homology with the Src family of intracellular tyrosine kinases², and includes putative SH3, SH2 and kinase domains (Fig. 2b). Several lines of evidence indicate that 27AIJA encodes a novel member of this gene family. First, the unique, amino-terminal domain of 27AIJA resembles that of two amniote family members, Lyn and Hck, almost equally (26% and 31% similarity, respectively)². Second, the complete coding sequence of 27AIJA is more than twice as divergent from its closest amniote relative (Hck, 38–40%) than are the sequences of other cloned *Xenopus* Src-family genes (*Xsrc*, *Xyes*, *Xfyn*, *Xlyn*) from their amniote homologues (3–18% (ref. 2; Xlyn sequence ID no. 2114076)). Finally, 27AIJA is less closely related to amniote Hck (38–40% divergence) than is the putative *Xenopus* homologue of the related Lyn gene (31–34% divergence). Thus, 27AIJA encodes a novel factor that can induce posterior, ectopic axes; we have named this gene *laloo*, after a nineteenth-century circus performer who had a small, headless twin protruding from his breastbone.

To better define the embryonic function of *laloo*, we tested its activity in ectodermal explant (animal cap) assays. At midgastrula stages, reverse transcription in conjunction with polymerase chain reaction (RT-PCR) revealed that *laloo*-injected caps express both *Xbra*, a pan-mesodermal marker, and *Xwnt8*, a marker of ventro-lateral mesoderm^{3,4}, but not *chordin*, a dorsal mesodermal marker⁵ (Fig. 3a, lanes 1–4). At late neurula stages, *laloo*-expressing caps show strong expression of *HoxB9* (*XlHbox6*), which at this stage is

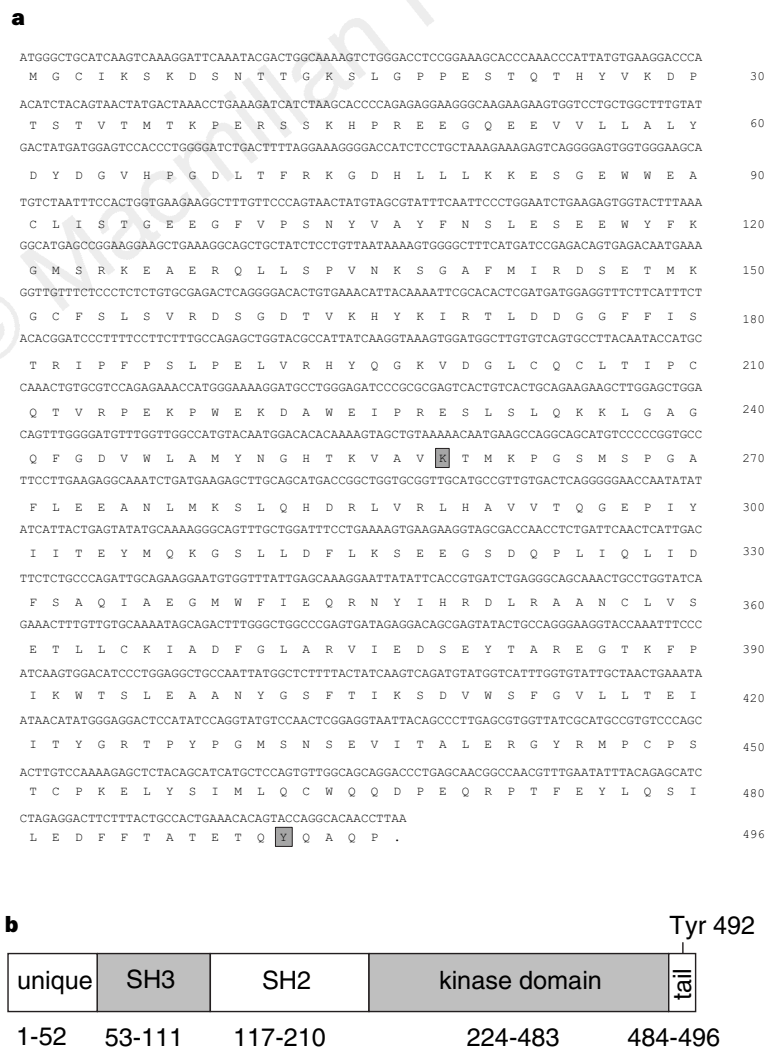


Figure 2 *laloo* is a novel Src-related gene. **a**, Nucleotide sequence and predicted open reading frame of *laloo*. Residues mutated in this study (K259, Y492) are boxed. **b**, Schematic of the Laloo protein tyrosine kinase. The *Xenopus* Laloo

protein is drawn approximately to scale, showing the positions of domains conserved throughout the Src gene family.

expressed in both lateral mesoderm and the spinal cord⁶ (Fig. 3b, lanes 1–4). Because NCAM, a pan-neural marker⁷, is not induced, we conclude that the *HoxB9* expression induced by Laloo at this stage represents mesodermal tissue. At high doses, Laloo induces the expression of *muscle actin*, a marker of paraxial mesoderm⁸ (Fig. 3b; lane 1); this result demonstrates that high levels of Laloo expression give rise to more dorsal fates than do lower doses. Figure 3c shows that Laloo also induces mesodermal markers in the context of the whole embryo at gastrula stages. Whereas control embryos express *Xbra* in a ring at the marginal zone at midgastrula stages, animal

pole injections of *laloo* RNA give rise to ectopic *Xbra* expression in the animal pole (39%, $n = 18$; Fig. 3c). These data indicate that overexpression of Laloo induces mesoderm, both in the animal cap assay and *in vivo*.

Mesoderm induction in *Xenopus* occurs between cleavage and early gastrula stages¹; *laloo* is expressed throughout this period (Fig. 3d). *laloo* RNA is present maternally; this early expression is, however, greatly diminished by late gastrula stages. Zygotic *laloo* expression initiates after late neurula stages. Using a combination of whole-mount *in situ* hybridization and microdissection techniques, we observed no tissue-specific localization of *laloo* RNA through neurula stages (not shown). The ubiquitous, early expression of this gene is consistent with a role for *laloo* in endogenous mesoderm induction.

Members of both the TGF- β and FGF ligand families have been shown to be capable of inducing mesoderm¹. We sought to determine whether mesoderm induction by Laloo is mediated through the signal transduction pathways downstream of these ligands. The intracellular Smad proteins transduce signals from activated TGF- β receptors; Smad4 has a central role in this process⁹. A truncated Smad4 molecule (tSmad4) has been shown to block mesoderm induction by both Smad1 and Smad2, signal transducers of the bone morphogenetic proteins and activin, respectively⁹. To test whether mesoderm induction by Laloo requires signalling through the Smad pathway, we co-expressed Laloo and tSmad4. As expected, co-injection of tSmad4 inhibits mesoderm induction by Smad2 (Fig. 3e, lanes 4 and 5). In contrast, tSmad4 does not block induction by Laloo (Fig. 3e, lanes 1 and 2). Thus, we conclude that the induction of mesoderm by Laloo acts downstream, or independently, of the Smad proteins.

The other intracellular pathway known to be involved in mesoderm induction acts through stimulation of the Ras/MAP kinase cascade, downstream of the FGF receptor^{10–17}. To determine whether Laloo induces mesoderm independently of the FGF pathway, we first co-expressed Laloo and a dominant-inhibitory form of Ras¹¹. Dominant-inhibitory Ras entirely blocks mesoderm induction by FGF (Fig. 3e, lanes 13 and 14), and also blocks induction by Laloo (Fig. 3e, lanes 9 and 11). This result indicates that mesoderm induction by Laloo requires signalling through the wild-type Ras protein. We then challenged Laloo activity with a truncated form of the FGF receptor (XFD), also shown to act as a dominant-inhibitory molecule¹⁰. We reasoned that, as a putative intracellular signalling molecule, Laloo might bypass an inhibition by XFD at the cell surface. XFD blocks *Xbra* and *Xwnt8* induction by FGF, as expected (Fig. 3e, lanes 21 and 22). Interestingly, XFD also blocks the induction of *Xbra* and *Xwnt8* by Laloo (Fig. 3e, lanes 17 and 19). These results indicate that Laloo is either part of the FGF pathway or in a parallel pathway that requires signalling through the FGF receptor and Ras.

All Src-family proteins contain a C-terminal tyrosine that, when phosphorylated, markedly inhibits the activity of the protein². To examine whether similar regulation of Laloo might occur during early *Xenopus* development, we constructed a mutant form of Laloo in which we replaced the putative negative regulatory tyrosine residue with phenylalanine (Y492F). Y492F is indeed a more potent mesoderm inducer than wild-type Laloo. At midgastrula stages, 50 pg of Y492F RNA is sufficient to induce *Xbra* and *Xwnt8* (Fig. 4a, lanes 1–4), whereas 250 pg of *laloo* RNA is required to induce expression of these markers (Fig. 3a, lanes 1–4). At late neurula stages, 50 pg of Y492F RNA induces *HoxB9* expression, and 250 pg induces expression of *muscle actin* (Fig. 4b, lanes 1–4); 250 pg and 2 ng, respectively, of *laloo* RNA is required to induce *HoxB9* and *muscle actin* expression (Fig. 3b, lanes 1–4). Thus, the mesoderm-inducing activity of Laloo is modulated through a C-terminal tyrosine residue. As shown earlier, both dominant inhibitory Ras (Fig. 4c, lanes 1 and 3) and XFD (Fig. 4c, lanes 1 and 4) block mesoderm induction by wild-type Laloo. On the other hand, while mesoderm induction by Y492F is blocked by dominant-inhibitory Ras (Fig. 4c, lanes 2 and 5), it is largely unaffected by

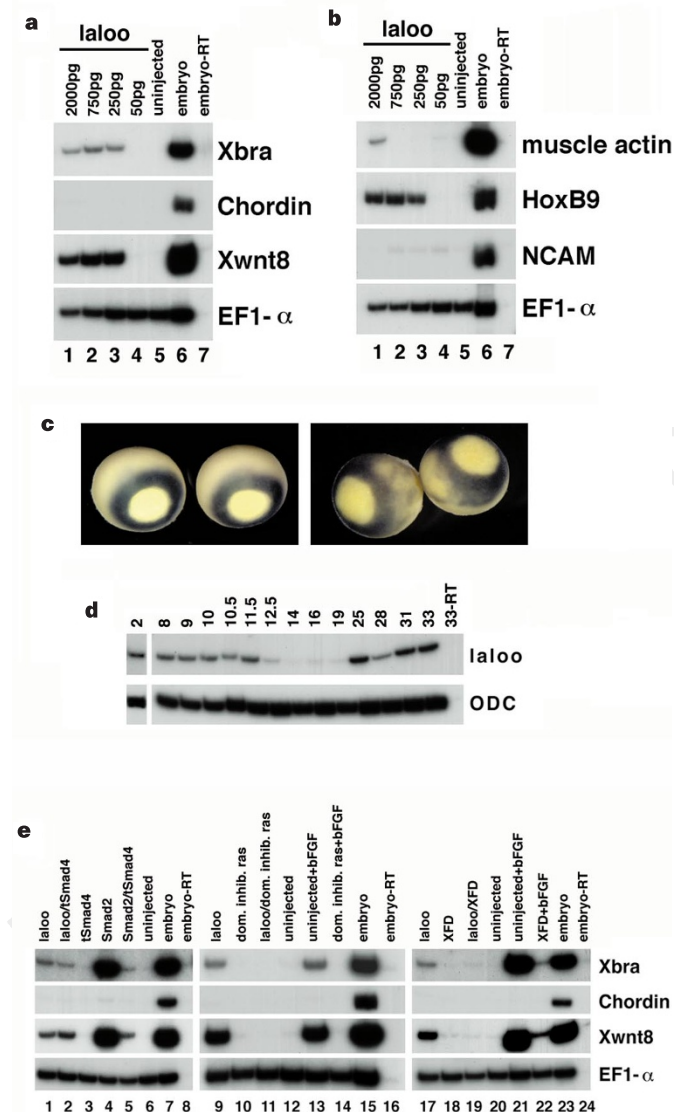


Figure 3 Ectopic Laloo induces mesoderm. RT-PCR analysis of animal caps dissected at late blastula stages and cultured until the stages listed. EF1- α is used as a loading control²⁹. The -RT lane contains all reagents except reverse transcriptase, and is used as a negative control. **a**, Analysis of animal caps cultured until midgastrula stages. Doses of *laloo* RNA over 2 ng were lethal. **b**, Analysis of animal caps cultured until late neurula stages. **c**, Whole-mount *in situ* hybridization of midgastrula stage embryos using an antisense *Xbra* probe. The embryos in the right panel were injected with 800 pg *laloo* RNA in the animal pole. **d**, Timing of *laloo* expression during early development. Ornithine decarboxylase (ODC) is used as a loading control³⁰. **e**, Induction of mesoderm by Laloo is unaffected by inhibition of Smad1 and Smad2, but is blocked by inhibition of the FGF signalling pathway. Animal caps were cultured until midgastrula stages. 750 pg each of *laloo*, *Smad2* and *tSmad4* RNA, 1.0 ng dominant-inhibitory Ras RNA and 1.5 ng XFD RNA were injected, as listed. Basic FGF (bFGF) was added to a final concentration of 25 ng ml⁻¹.

the co-expression of XFD (Fig. 4c, lanes 2 and 6). These results indicate that the requirement for FGF receptor activity is mediated through Tyr 492 of Lalloo; furthermore, these data implicate Lalloo as an integral component of the FGF signal transduction pathway, acting downstream of the FGF receptor and upstream of Ras.

In cell culture studies, kinase-defective mutants of Src-family members have been shown to act as dominant-negative molecules, blocking signalling through the wild-type kinase². We constructed a kinase-defective Lalloo mutant by disrupting the putative ATP phosphotransferase site². This mutant, K259E, does not induce either *Xbra* or *Xwnt8* in mid-gastrula ectoderm explants (Fig. 4d, lane 2), demonstrating that mesoderm induction by Lalloo requires a functional kinase domain. K259E expression inhibits mesoderm induction by Lalloo at four-fold concentrations over wild-type (Fig. 4d, lanes 1 and 3); moreover, this mutant can inhibit mesoderm induction by both bFGF and activin in animal cap assays. Expression of K259E blocks induction of both *Xbra* and *Xwnt8* by bFGF (Fig. 4d, lanes 6 and 8), and blocks induction of *Xbra*, but not *Xwnt8* or *chordin*, by activin (Fig. 4d, lanes 10 and 12). Coexpression of Lalloo moderately but consistently rescues mesoderm induction by FGF (Fig. 4d, lanes 6 and 7) and activin (Fig. 4d, lanes 10 and 11). This suggests that K259E acts by competition with wild-type Lalloo. Rescue can also be achieved by coexpression of constitutively active Ras (not shown; ref. 11), supporting the placement of Lalloo upstream of Ras in mesoderm induction. Marginal zone injections of K259E result in a reduction of trunk and tail structures *in vivo*

similar to that seen after injection of other molecules that disrupt the FGF signal transduction pathway^{10,12,14–16,18}; coexpression of either Lalloo or constitutively active Ras partly rescues axis formation (Fig. 4e). These results indicate that Lalloo, or a related factor inhibited by K259E, is required for mesoderm induction by FGF or activin and for normal development of the body axis.

Our results are consistent with a model placing Lalloo as an essential intermediate in the FGF signalling pathway, downstream of the FGF receptor and upstream of Ras. The block of activin-induced *Xbra* expression by K259E suggests that Lalloo might also mediate aspects of activin signalling; we believe, however, that this inhibition is indirect. Although FGF signalling is required for the full range of induction by activin, some activin-inducible genes are 'FGF-independent'; for example, *Xwnt8* is induced in XFD-expressing animal caps treated with activin^{13,19}. We have demonstrated both that K259E fails to block the induction of *Xwnt8* by activin and that Lalloo activity is unaffected by coexpression of tSmad4; thus, the inhibition of activin-induced *Xbra* expression by K259E is likely to be secondary to a block of FGF signalling.

Experiments with XFD and the hyperactive Lalloo construct Y492F suggest that mesoderm induction by Lalloo requires the FGF-mediated dephosphorylation of Y492. Interestingly, inhibition of SH2-containing protein tyrosine phosphatase 2 (SH-PTP2) blocks mesoderm induction by FGF²⁰. Thus, *in vivo*, the activated FGF receptor might activate SH-PTP2, or a related phosphatase, which in turn could activate Lalloo via dephosphorylation of Y492.

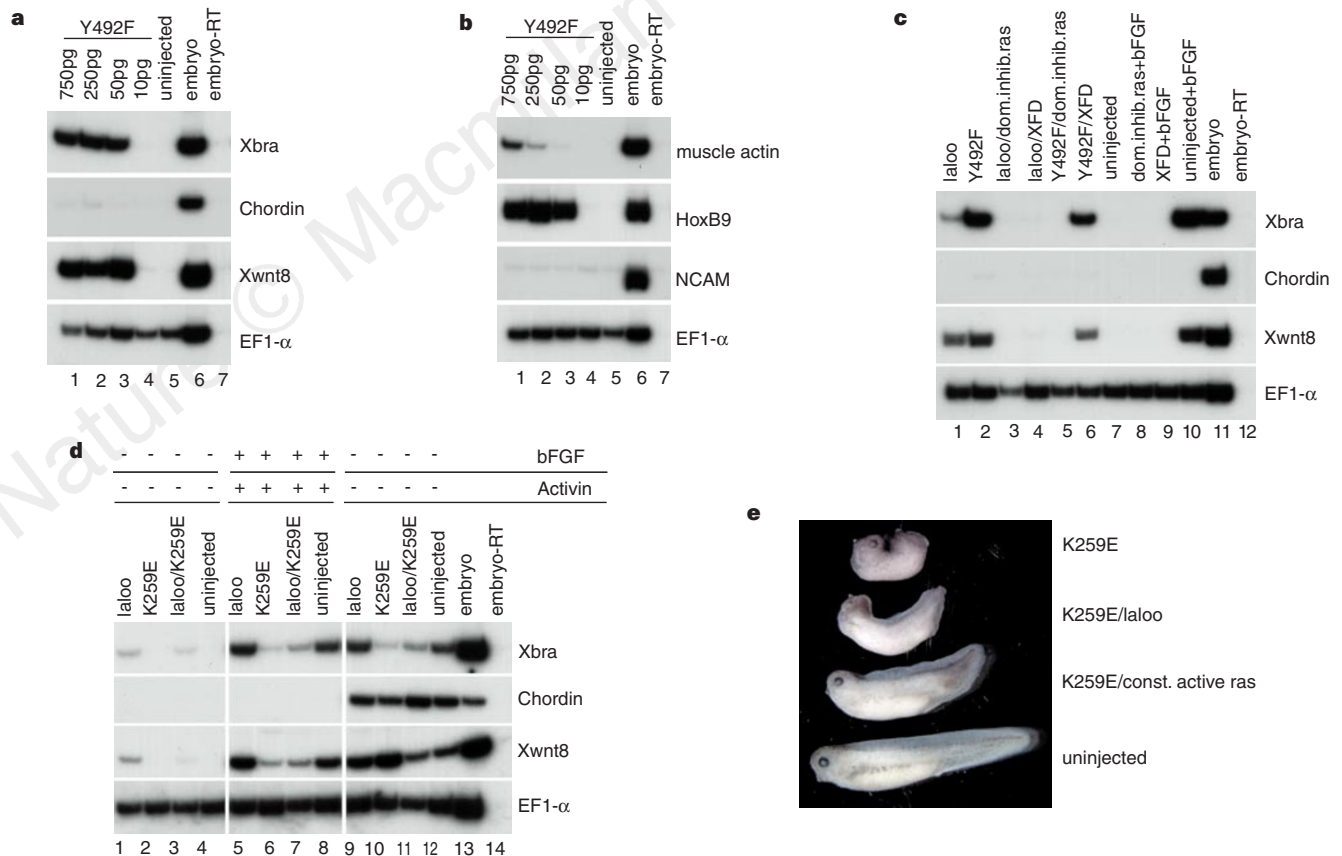


Figure 4 Y492F bypasses inhibition by XFD, and K259E inhibits the activity of mesoderm-inducing growth factors and normal development. Animal caps were cultured until midgastrula (**a**, **c**, **d**) or late neurula (**b**) stages. **a**, **b**, Y492F is a more potent mesodermal inducer than wild-type lalloo. **c**, A hyperactive lalloo mutant bypasses inhibition by the truncated FGF receptor. 750 pg lalloo, 250 pg Y492F, 1.0 ng dominant-inhibitory Ras and 1.5 ng XFD were injected. **d**, K259E inhibits mesoderm induction by bFGF and activin. 800 pg lalloo and 3.2 ng K259E RNA were injected. Inhibition by K259E required doses of 3.2 ng or more. **e**, K259E perturbs normal development of the body axis. Lateral view of stage 37 embryos;

2 ng K259E, 400 pg lalloo and 40 pg activated Ras RNA were injected radially, as listed, at early cleavage stages. Top, embryo injected with K259E RNA. 81% of these embryos display a failure of blastopore closure and a complete loss of tail structures ($n = 78$). Second from top, embryo injected with both K259E and lalloo RNA (56% with posterior truncations; $n = 70$). These embryos often show a reduction of anterior structures. Second from bottom, embryo injected with both K259E and constitutively active Ras RNA (33% with posterior truncations, $n = 64$). Bottom, uninjected control embryo.

Our results also suggest that the activity of ectopic *Laloo* is dependent upon a basal level of signalling through the FGF receptor. In support of this, it has been shown that FGF receptor-dependent MAP kinase activity is present throughout the early *Xenopus* embryo²¹. It has also been demonstrated that an autoregulatory loop involving FGF is required for mesoderm maintenance^{18,22,23}; Y492F might thus generate ectopic mesoderm in the presence of XFD by bypassing the requirement for continued signalling through the FGF receptor.

The positioning of Src-related factors between the FGF receptor and Ras has precedents in other studies. Src-family kinases have previously been shown to transmit signals through Ras; the molecular interactions proposed to link these factors include phosphorylation of Shc and/or Ras GTPase-activating protein². Functional association between Src-related proteins and receptor tyrosine kinases has also been demonstrated²⁴. Our studies do not, however, address whether signalling upstream of *Laloo* is mediated solely through the FGF receptor; *Laloo* might also receive input from other cell-surface receptors. Furthermore, redundancy has been demonstrated among Src-family genes in other biological contexts²; mesoderm induction *in vivo* might thus involve additional Src-related factors. Although a constitutively active form of chicken Src has been reported not to induce mesoderm in *Xenopus* explants¹³, this apparent difference might be due to cross-species incompatibility as well as to differences in assay conditions. Efforts are currently in progress to address these possibilities. This report provides strong evidence of a critical role for a Src-family kinase in early vertebrate development, acting as a required component of the FGF signal transduction pathway. □

Methods

Expression library construction and screening. Early gastrula (stage 10) *Xenopus laevis* embryos were homogenized with RNazol B solution and processed in accordance with the manufacturer's instructions (Tel-Test). 4.5 µg poly(A)⁺ RNA was selected from 2.4 mg total RNA using the Oligotex mRNA midi kit (Qiagen). cDNA synthesis and linker addition was performed using the Superscript II unidirectional kit (Gibco BRL). After second-strand synthesis, cDNAs were size-selected by gel filtration (average size 2.0 kb) and directionally subcloned into the *SalI* and *NotI* sites of a modified pCS2 vector. 2 × 10⁶ transformants were obtained after electroporation in ElectroMAX DH10B cells (Gibco BRL).

The library was plated to obtain initial fractions of approximately 200 clones. Similar functional screens in *Xenopus*, using small pools of RNAs, have been described elsewhere²⁵. For subsequent sib selection, 10 pools of fivefold fewer clones were screened (e.g. 10 × 40, 10 × 8). Pooled plasmid DNA was isolated using the QIAprep spin miniprep kit (Qiagen) and linearized with *AscI*. Capped RNA was synthesized using the mMessage mMachine kit (Ambion). Embryos were injected with 10 nl/blastomere of 0.5 mg ml⁻¹ RNA into animal poles of both blastomeres at the two-cell stage, and cultured until tadpole stages.

RNA preparation, explant dissection and cell culture. *laloo* RNA and all mutant derivatives contained the *laloo* open reading frame, as well as 84 nucleotides of 5' and 34 nucleotides of 3' untranslated sequence. All mRNA was synthesized *in vitro* in the presence of cap analogue using the mMessage mMachine kit. Microinjection, explant dissection and culture were performed as described²⁶. Recombinant bFGF was obtained from Boehringer Mannheim.

Whole-mount immunohistochemistry, β-Gal detection and *in situ* hybridization. Whole-mount antibody staining was performed as described²⁶. The 6F11 antibody was used at 1:1 dilution, and the 12/101 antibody was used at 1:500 dilution. Secondary antibody was a donkey anti-mouse IgG coupled to horseradish peroxidase (Jackson Laboratories) and was used at 1:250 dilution. Colour reactions were performed using the DAB and Vector SG kits (Vector Laboratories). Whole-mount β-Gal detection and hybridization *in situ* were performed as described⁴. The antisense *Xbra* probe was synthesized in the presence of digoxigenin-11-UTP (Boehringer Mannheim).

RT-PCR. RT-PCR was performed as described⁹. Primers constructed for this study were as follows: *laloo* (forward, 5'-TGGCTCTGTACTGTGATC; reverse, 5'-GTCATACAAAGCCAGCAG); *chordin* (forward, 5'-CAGTCAGATGGAG-CAGGATC; reverse, 5'-AGTCCCATTGCCCGAGTTGC); *ODC* (forward, 5'-

AATGGATTCAGAGACCA; reverse, 5'-CCAAGGCTAAAGTTGCG). All other primer sequences were as described²⁶. PCR for *laloo*, *Xwnt8*, *HoxB9* and *NCAM* were performed for 25 cycles; PCR for *EF1-α*, *Xbra*, *chordin*, *muscle actin* and *ODC* were performed for 21 cycles.

Preparation of *laloo* mutant constructs. The *laloo* mutants K259E and Y492F were generated by PCR. For K259E, we introduced a point mutation (A → G) that resulted in a lysine (AAA) to glutamic acid (GAA) mutation in the resulting construct. The oligonucleotide used for this mutagenesis was as follows: 5'-GTA GAA ACA ATG AAG CCA GGC AGC. For Y492F, we introduced a point mutation (A → T) that resulted in a tyrosine (TAC) to phenylalanine (TTC) mutation in the resulting construct. The complementary strand oligonucleotide thus includes a T → A mutation: 5'-TTA AGG TTG TGC CTG GAA CTG.

Received 10 March; accepted 26 June 1998.

1. Klein, P. S. & Melton, D. A. Hormonal regulation of embryogenesis: the formation of mesoderm in *Xenopus laevis*. *Endocr. Rev.* **15**, 326–341 (1994).
2. Brown, M. T. & Cooper, J. A. Regulation, substrates and functions of src. *Biochim. Biophys. Acta* **1287**, 121–149 (1996).
3. Smith, J. C., Price, B. M. J., Green, J. B. A., Weigel, D. & Herrmann, B. G. Expression of a *Xenopus* homolog of Brachyury (T) is an immediate-early response to mesoderm induction. *Cell* **67**, 79–87 (1991).
4. Smith, W. C. & Harland, R. M. Injected *Xwnt-8* RNA acts early in *Xenopus* embryos to promote formation of a vegetal dorsolateral center. *Cell* **67**, 753–765 (1991).
5. Sasai, Y., Lu, B., Steinbeisser, H., Geissert, D., Gont, L. K. & DeRobertis, E. M. *Xenopus* chordin: a novel dorsolateralizing factor activated by organizer-specific homeobox genes. *Cell* **79**, 779–790 (1994).
6. Wright, C. V. E., Morita, E. A., Wilkin, D. J. & DeRobertis, E. M. The *Xenopus* X1Hbox6 homeo protein, a marker of posterior neural induction, is expressed in proliferating neurons. *Development* **109**, 225–234 (1990).
7. Kintner, C. R. & Melton, D. A. Expression of *Xenopus* NCAM RNA in ectoderm is an early response to neural induction. *Development* **99**, 311–325 (1987).
8. Mohun, T. J., Brennan, S., Dathan, N., Fairman, S. & Gurdon, J. B. Cell type-specific activation of actin genes in the early amphibian embryo. *Nature* **311**, 716–721 (1984).
9. Lagna, G., Hata, A., Hemmati-Brivanlou, A. & Massague, J. Partnership between DPC4 and SMAD proteins in TGF-β signalling pathways. *Nature* **383**, 832–836 (1996).
10. Amaya, E., Musci, T. J. & Kirschner, M. W. Expression of a dominant negative mutant of the FGF receptor disrupts mesoderm formation in *Xenopus* embryos. *Cell* **66**, 257–270 (1991).
11. Whitman, M. & Melton, D. A. Involvement of p21^{ras} in *Xenopus* mesoderm induction. *Nature* **357**, 252–255 (1992).
12. MacNicol, A. M., Muslin, A. J. & Williams, L. T. Raf-1 kinase is essential for early *Xenopus* development and mediates the induction of mesoderm by FGF. *Cell* **73**, 571–584 (1993).
13. LaBonne, C. & Whitman, M. Mesoderm induction by activin requires FGF-mediated intracellular signals. *Development* **120**, 463–472 (1994).
14. LaBonne, C., Burke, B. & Whitman, M. Role of MAP kinase in mesoderm induction and axial patterning during *Xenopus* development. *Development* **121**, 1475–1486 (1995).
15. Gotoh, Y., Masuyama, N., Suzuki, A., Ueno, N. & Nishida, E. Involvement of the MAP kinase cascade in *Xenopus* mesoderm induction. *EMBO J.* **14**, 2491–2498 (1995).
16. Umbhauer, M., Marshall, C. J., Mason, C. S., Old, R. W. & Smith, J. C. Mesoderm induction in *Xenopus* caused by activation of MAP kinase. *Nature* **376**, 58–62 (1995).
17. Northrop, J. *et al.* BMP-4 regulates the dorsal-ventral differences in FGF/MAPKK-mediated mesoderm induction in *Xenopus*. *Dev. Biol.* **172**, 242–252 (1995).
18. Amaya, E. & Kroll, K. L. Transgenic *Xenopus* embryos from sperm nuclear transplantations reveal FGF signaling requirements during gastrulation. *Development* **122**, 3173–3183 (1996).
19. Cornell, R. A. & Kimmel, D. Activin-mediated mesoderm induction requires FGF. *Development* **120**, 453–462 (1994).
20. Tang, T. L., Freeman, R. M. Jr, O'Reilly, A. M., Neel, B. G. & Sokol, S. Y. The SH2-containing protein-tyrosine phosphatase SH-PTP2 is required upstream of MAP kinase for early *Xenopus* development. *Cell* **80**, 473–483 (1995).
21. LaBonne, C. & Whitman, M. Localization of MAP kinase activity in early *Xenopus* embryos: implications for endogenous FGF signaling. *Dev. Biol.* **183**, 9–20 (1997).
22. Isaacs, H. V., Pownall, M. E. & Slack, J. M. W. eFGF regulates *Xbra* expression during *Xenopus* gastrulation. *EMBO J.* **13**, 4469–4481 (1994).
23. Schulte-Merker, S. & Smith, J. C. Mesoderm formation in response to Brachyury requires FGF signaling. *Curr. Biol.* **5**, 62–67 (1995).
24. Parsons, J. T. & Parsons, S. J. Src family protein tyrosine kinases: cooperating with growth factor and adhesion signaling pathways. *Curr. Opin. Cell Biol.* **9**, 187–192 (1997).
25. Lustig, K. D., Kroll, K. L., Sun, E. E. & Kirschner, M. W. Expression cloning of a *Xenopus* T-related gene (Xombi) involved in mesodermal patterning and blastopore lip formation. *Development* **122**, 4001–4012 (1996).
26. Hemmati-Brivanlou, A. & Melton, D. A. Inhibition of activin receptor signaling promotes neuralization in *Xenopus*. *Cell* **77**, 273–281 (1994).
27. Harris, W. A. & Hartenstein, V. Neuronal determination without cell division in *Xenopus* embryos. *Neuron* **6**, 499–515 (1991).
28. Kintner, C. R. & Brockes, J. P. Monoclonal antibodies identify blastemal cells derived from dedifferentiating muscle in newt limb regeneration. *Nature* **308**, 67–69 (1984).
29. Krieg, P., Varnum, S., Wormington, M. & Melton, D. A. The mRNA encoding elongation factor 1α (EF-1α) is a major transcript at the mid-blastula transition in *Xenopus*. *Dev. Biol.* **133**, 93–100 (1989).
30. Bassez, T., Paris, J., Omilli, F., Dorel, C. & Osborne, H. B. Post-transcriptional regulation of ornithine decarboxylase in *Xenopus laevis* oocytes. *Development* **110**, 955–962 (1990).

Acknowledgements. We thank M. Whitman and E. Amaya for providing us with the Ras and XFD constructs, respectively; W. Harris for the 6F11 antibody; and members of the laboratory, P. Wilson and H. Hanafusa, for critical reading of the manuscript. F.C. received partial financial support from Programma Scambi Internazionali and Piano Bilaterale of CNR of Rome. A.H.-B. is a Merck and a McKnight scholar. This work was supported by NIH grant HD 32105-01 and by grants from the Klingenstein and Merck Foundations to A.H.-B.

Correspondence and requests for materials should be addressed to A.H.-B. (e-mail: brvnlou@rockvax.rockefeller.edu). The GenBank accession number for *laloo* is AF081803.